Available online at www.sciencedirect.com
SCIENCE DIRECT
Journal of the European Ceramic Society 26 (2006) 1707–1713
www.elsevier.com/locate/jeurceramsoc

Densification of liquid phase sintered silicon carbide

A. Can [a], M. Herrmann [b,*], D.S. McLachlan [a], I. Sigalas [a], J. Adler [b]

[a] *University of Witwatersrand, Johannesburg, South Africa*
[b] *Fraunhofer Institute of Ceramic Technologies and Sintered Materials, Dresden, Germany*

Received 22 January 2005; received in revised form 8 March 2005; accepted 19 March 2005
Available online 3 June 2005

Abstract

The densification and phase formation of liquid phase sintered silicon carbide (LPSSiC) with 10 wt.% additives were investigated. The ratio of the Al_2O_3/Y_2O_3-additives was changed between 4:1 and 1:2. Densification was carried out by hot pressing and gas pressure sintering. The different densification routes result in different major grain boundary phases—aluminates in gas pressure sintered materials and silicates in hot pressed samples. Thermodynamic calculations were carried out to determine the amount of liquid phase during densification and for the interpretation of the results.

Keywords: SiC; Carbides; Sintering; Microstructure; Grain boundary

1. Introduction

Silicon carbide is a preferred ceramic material for many applications in harsh environmental conditions because of its resistance to high temperatures, aggressive chemicals and abrasion.[1] The sintering of SiC (SSiC) is usually performed at very high temperatures up to 2200 °C in the solid state, with small amounts of boron, carbon, or aluminium as additives. In the recent years, liquid phase silicon carbide LPSSiC has been developed as a material with a higher fracture toughness than the SSiC but with a similar hardness. The use of yttria or other rare earth oxides and Al_2O_3 or AlN as sintering additives, which form, together with the SiO_2 existing on the surface of the starting SiC-powder, a liquid phase during the sintering, reducing the sintering temperature to values less than 2000 °C,[1,2] in comparison to 2100–2200 °C for solid phase sintered SiC (SSiC).

However, a major problem associated with sintering of silicon carbide in the presence of oxide additives is the reaction between the silicon carbide and the oxides.[3–9] The major weight loss in the $SiC–Al_2O_3–Y_2O_3$-system during sintering is a result of the formation of gaseous CO, SiO, Al_2O and Al.[3,5,6]

The sintering conditions influence the composition of the gaseous phases formed and consequently the extent of the mass losses.[3–6,10,11] If not properly controlled, the resultant mass loss can significantly affect the final properties of the materials. Therefore, it is a common practice to use a powder bed to minimise the mass loss by gas forming reactions during the sintering of LPSSiC. In most cases a mixture of SiC and Al_2O_3 are used for the powder bed.[6,10,11] In most previous investigations the influence of the SiO_2 on the densification and properties is neglected after the statement that the SiO_2 is the less stable component and will evaporate at low temperatures. They then focus more on the decomposition reactions of Al_2O_3 and Y_2O_3.[6–8] Therefore, the influence of the SiO_2-content on the amount of liquid and hence on the densification is not yet studied in detail. Also most of the research work in the literature[10–15] has focused on only a few parameters, such as the polytype and grain size of the starting silicon carbide powders. The aim of this paper is to show the influence of the SiO_2 and the Al_2O_3/Y_2O_3 ratio, based on a comparison of the densification of hot pressed and gas pressure sintered

* Corresponding author.
E-mail address: herrmann@ikts.fraunhofer.de (M. Herrmann).

0955-2219/$ – see front matter © 2005 Published by Elsevier Ltd.
doi:10.1016/j.jeurceramsoc.2005.03.253

samples. Thermodynamic calculations of the amount of liquid phase, which depend on temperature and SiO_2-content of the materials, were carried out as part of the explanation of the results.

2. Experimental

The samples were prepared starting from α-SiC (UF15) and 10 wt.% mixed Al_2O_3 (Alcoa A16 SG) and Y_2O_3 (H.C. Starck grade C) additives. The SiO_2 content in the starting powder was 1.7 wt.%. The composition of additives was changed in a systematic way varying the mol ratio from 4 Al_2O_3/1 Y_2O_3 to 4 Y_2O_3/1 Al_2O_3 (Table 1). The powders were first mixed in isopropanol in a planetary ball mill for 2 h. The isopropanol used contains 0.5 wt.% triethylene glycol and 3.0 wt.% Triton-X100 for better dispersing and shaping. Samples (dimensions: 100 mm × 20 mm × 20 mm) were cold isostatically pressed at 250 MPa for gas pressure sintering experiments.

Burning out prior to hot pressing was done in an air furnace at 450 °C for 1 h (with a ramping cycle of 5 °C/min) in porcelain crucibles. In the case of the cold-isostatically pressed bars, used in gas pressure sintering, organic additives were removed at 1100 °C in an Ar atmosphere.

The hot pressing of the samples was carried out at 1975 °C for 30 min, under 30 MPa (HPW200/250, company KCE/FCT), using ramp rate of 10 K/min and an Ar pressure of 1 bar. The final dimension of the samples was Ø 80 and 6 mm height.

The CIPed samples were gas pressure sintered using two cycles with different heating rates. For cycle I a heating rate of 5 K/min up to 1875 °C was used. At 1875 °C there was a holding time of 30 min. During the subsequent 5 K/min ramp up to 1925 °C the Ar pressure was raised from 1 to 80 bar. The final sintering was carried out at 1925 °C for 60 min, under a gas pressure of 80 bar (8 MPa). The cycle II differed from cycle I in the heating rate, in this case it was 10 K/min. Graphite crucibles were used for the sintering of all the samples. No powder bed was used. The densities were measured by the Archimedes method. After sintering the samples were cut into slices with dimensions of 20 mm × 20 mm × 5 mm for further investigations. All investigations were made on 20 mm × 20 mm cross sectional faces. The phase composition of the samples was determined by X-ray diffraction analysis (XRD 7; Seifert-FPM; Cu Kα), using JCPDS standards.[16] The theoretical density was determined using the density of the starting components and the equation:

$$\rho = \frac{100}{\sum m_i/\rho_i}$$

where m_i is the mass fraction in wt.% and ρ_i density of the starting components.

The microstructures of polished surfaces were examined using both an optical microscopy and a scanning electron microscopy, with an attached EDX (Leica Stereoscan 260).

The Young's modulus was determined by standard ultrasonic run time measurements.

The FactSage® software package was used for thermodynamic calculations.[17] The necessary thermodynamic data for the calculations were taken from the SGTE (Scientific Group Thermodata Europe) pure substance database (SGPS)[18] and the solution database (SGSL),[19] as well as the special data set of the system Y–Al–Si–C–O from SGTE[20] based on the data set of Groebner.[21] For the modelling of the melt a partial ionic liquid model was used.[21] The oxide phases, oxycarbide phase and carbide phases were used for the calculation. The quartz and tridymite phases were all excluded because the automatic extrapolation of the data outside the stability area (in the area of higher temperatures) results in some troubles. The gaseous species were taken into account up to a pressure of 10^{-70} atm. The amount of the gas phase was less 1 wt.% of the overall mass. Therefore no significant change in the composition of the condensed phases takes place. The calculations were carried out at constant pressure of 1 atm. The calculated phase diagram[21] is in good agreement with the experimental data.[25]

Table 1
The composition, phase content and measured density (ρ) observed after hot pressing and gas pressure sintering

Material			Hot pressed at 1975 °C				Gas pressure sintered at 1925 °C		
Name	Al_2O_3/Y_2O_3 (mol/mol)[a]	Phases formed at equilibrium (calculated)	T_m	Density (g/cm^3)	ρ/ρ_{th} (%)	Crystalline grain boundary phase[b,c]	Density (g/cm^3)	ρ/ρ_{th} (%)	Crystalline grain boundary phase[b,c]
4Al 1Y	4:1	YAG; mullite, $Y_2Si_2O_7$	1400	3.27	100	$Y_2Si_2O_7$, Al_2O_3	3.26	97.6	YAG, Al_2O_3
5Al 3Y	5:3	YAG; mullite, $Y_2Si_2O_7$	1400	3.26	99.4	YAG (s)	3.30	98.6	YAG
1Al 1Y	1:1	YAG, $Y2Si_2O_7$; mullite	1400	3.27	99.4	$Y_2Si_2O_7$, YAG	3.32	98.8	YAG/YAM
1Al 2Y	1:2	Y_2SiO_5, $Y2Si_2O_7$, YAG	1425	3.30	100.3	Y_2SiO_5, YAG	3.27	97.0	YAM, YAP, YAG (s)
1Al 4Y	1:4	Y_2SiO_5, YAM, YAG	1727	3.31	100.3	Y_2SiO_5	3.05	90.5	Not measured

The theoretical density ρ_{th} of the hot pressed samples was calculated under the assumption that all the SiO_2 remains in the sample; the theoretical density of the gas pressured materials were calculated under the assumption, that all SiO_2 was evaporated, T_m—temperature of melt formation from the phase diagram calculated after [21].

[a] Initial SiO_2 content 1.7 wt.%.

[b] YAG- compound composition $Y_3Al_5O_{12}$; YAM-compound composition $Y_4Al_2O_9$; YAP–$YAlO_3$; (s) observed only small amounts.

[c] Determined by XRD.

3. Results

The densification and the densification rates during hot pressing of the samples are given in Fig. 1. As can be seen with decreasing Al_2O_3/Y_2O_3 mol ratio the densification starts at higher temperatures. Note that for the sample with 1:4 Al_2O_3/Y_2O_3 ratio the first peak of the densification rate is only a shoulder of the main peak of the densification rate. The start of the rapid densification of all samples correlates well with the temperature at which the melt is formed (Table 1). The melting point of the grain boundary phase could be determined from the phase diagram (Fig. 2). For convenience the starting compositions of the grain boundary phases are shown in the phase diagram. These were calculated assuming the SiO_2 content to be 1.7 wt.%, of the starting mixture.

The density and phase composition of the samples is given in Table 1. In spite of the differences in the densification behaviour, all samples were almost completely densified using hot pressing. The densities higher than 99.5% theoretical density could be confirmed by the analysis of polished cross sections. The relative densities of the hot pressed samples in Table 1 were calculated assuming, that no SiO_2 evaporated as SiO and CO during the densification. Evidence, that most of the SiO_2 remains in the sample is confirmed by a XRD analysis of the hot pressed samples. Silicates as well as aluminates are formed. Not all of the predicted silicates are detected (compare columns 3 and 7, Table 1), which can be explained by the formation of amorphous phases, which are typical for the SiO_2–Y_2O_3–Al_2O_3 system.

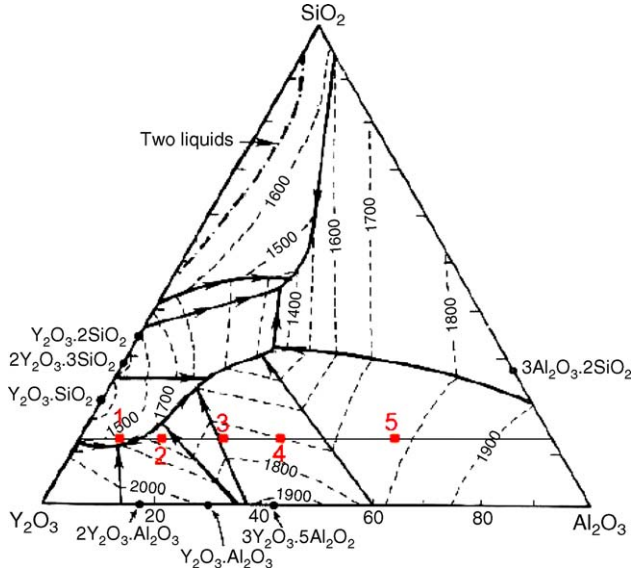

Fig. 2. Liquidus surface of the Y_2O_3–Al_2O_3–SiO_2 phase diagram [25]. Included are the starting compositions of the sintering additives (including the SiO_2 content of the SiC-powder 1.7 wt.%).

The density and the weight losses for the two different sintering cycles are shown in Fig. 3, while only the densities and phase composition of the samples sintered using cycle I are given in Table 1. The samples with the high Al_2O_3/Y_2O_3 additive ratio showed the higher weight losses. Nevertheless these samples could be sintered to densities higher than 98% theoretical density. The samples with an Al_2O_3/Y_2O_3 ratio less than 1:1 could not be completely densified independent of the sintering cycle (A or B).

It should be noted that for the GPS samples, with high Al_2O_3 contents, the absolute values of the densities are higher than those of the hot pressed samples, with the same starting compositions. This is due to the evaporation of the SiO_2 in

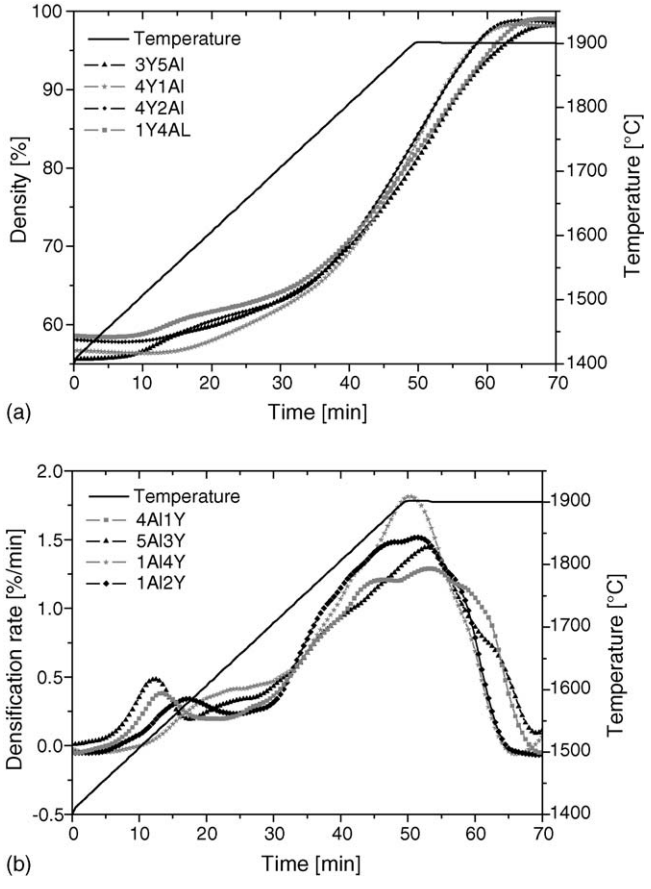

Fig. 1. Densification (a) and densification rate (b) during hot pressing for the different compositions. (1Y 4Al means a sample with additive mol ratio 4 Al_2O_3/1 Y_2O_3).

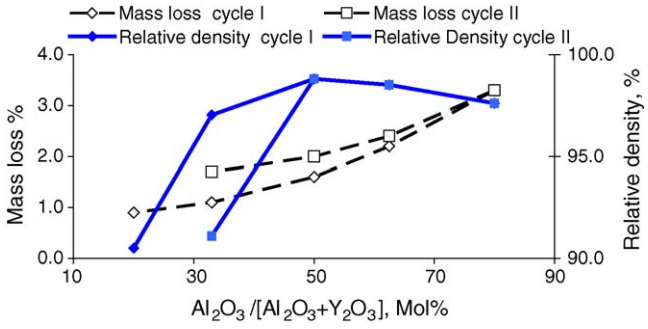

Fig. 3. Dependence of the relative density and of the mass loss of LPSSiC-materials with 10 wt.% additives and different ratios for sintering cycles I and II.

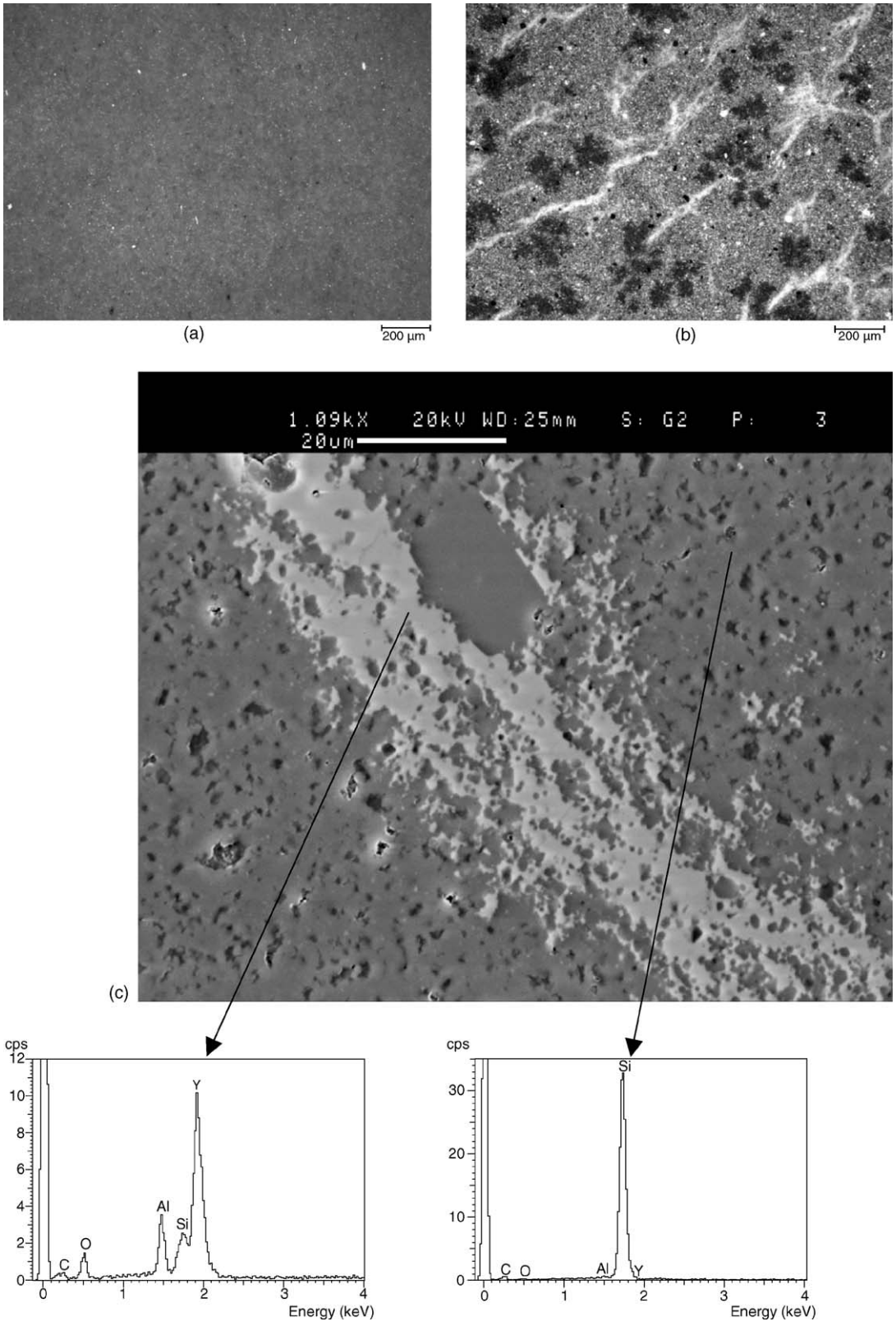

Fig. 4. Dark field image of hot pressed (a) and gas pressure sintered (b) and detailed SEM figure with the resulting EDX analysis of the gas pressure sintered (c) materials with a Al_2O_3/Y_2O_3 additive mol ratio of 1:2.

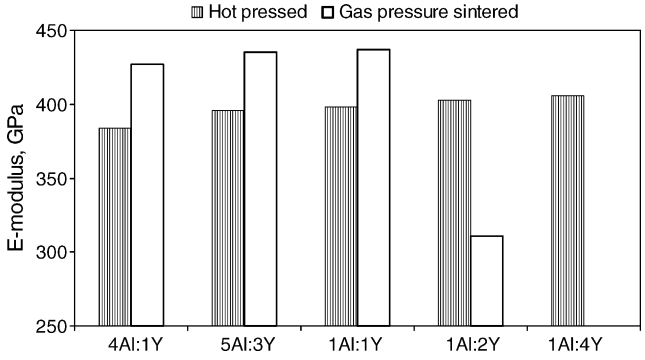

Fig. 5. E-modulus of the gas pressure sintered and hot pressed materials.

the gas pressure sintered materials and the formation of only aluminates at the crystalline grain boundaries (Table 1). The theoretical density for these samples was calculated under the assumption that all SiO_2 evaporated. Therefore the calculated relative densities for the gas pressure sintered samples are at the lower bound. Indeed, the analysis of the polished section showed, the samples with Al_2O_3/Y_2O_3 ratio ≥ 1 had porosities of less than 1%. Large areas, enriched with Y_2O_3, were found in the gas pressure sintered sample, with an additive ratio Al_2O_3/Y_2O_3 of 1:2, using SEM. The hot pressed samples of the same composition showed no such segregation (Fig. 4). The reasons of the segregations will be outlined in another paper.[22]

The same ratios of the α-SiC polymorphs were found in the hot pressed and gas pressure sintered samples with the different additive ratios.

The results of ultrasonic measurements are given in Fig. 5. Differences between hot pressed and gas pressure sintered samples were observed. For the samples, which could be densified with both methods to a density higher than 98%, the E-modulus of the gas pressure sintered materials are higher than those of the hot pressed ones. This could be explained by the higher elastic constants of the aluminates compared with that of the silicates and the glassy grain boundaries existing in hot pressed samples. This is additional evidence for the different nature of the grain boundary phases in the hot pressed and the gas pressure sintered materials.

4. Discussion

The results of the densification experiments showed that the densification of the hot pressed and gas pressure sintered materials are very different as are the resulting compositions and microstructures of the materials themselves. The main reason for this is, that during hot pressing the evaporation of the formed oxide liquid phases will be minimised. The reduced evaporation is connected with two facts: first, it is caused by the faster densification due to the additional driving force (30 MPa applied mechanical pressure). The second reason is that the mould which is used for hot pressing is nearly closed resulting in small amount of gas phase. Therefore, only few amounts have to evaporate to reach the local equilibrium. A more extensive evaporation of the SiO_2 dissolved in the liquid phase takes place during gas pressure sintering due to the larger effective volume of the furnace and the much longer period up to the moment where no open porosity exist. The compositions of the gas phase over a LPSSiC material with 10 wt.% additives and a Al_2O_3/Y_2O_3 additive mol ratio of 4:1 were calculated for better understanding of the evaporation. The calculations showed, that both the CO- and SiO-partial pressure were highest in materials with large amounts of SiO_2 (Fig. 6a), indicating a large evaporation according reaction:

$$SiC\,(s) + 2SiO_2\,(l) \leftrightarrow 3SiO + CO\,(g) \quad (1)$$

These calculated partial pressures increase by more than a factor of 10 when the temperature increases from 1500 to 1700 °C. Similar behaviour was determined by the determination of the weight loss during the heating[24] and by mass spectroscopic measurements of the composition of the gas phase during the sintering of SiO_2 rich LPSSiC materials.[12]

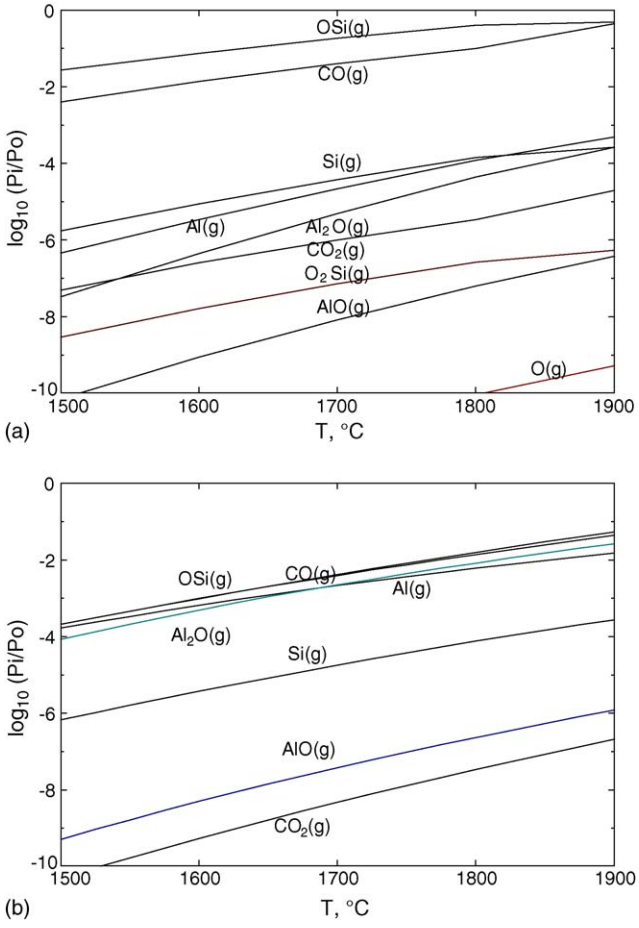

Fig. 6. Calculated partial pressures (P_i/P_0; $P_0 = 0.1$ MPa) over LPSSiC material with 10 wt.% additives mol ratio of the additives $Al_2O_3/Y_2O_3 = 4:1$ and additional 2 wt.% SiO_2 (a) and without remaining SiO_2 (b) as a function of temperature (changes in the slope are connected with appearing or disappearing of condensed phases).

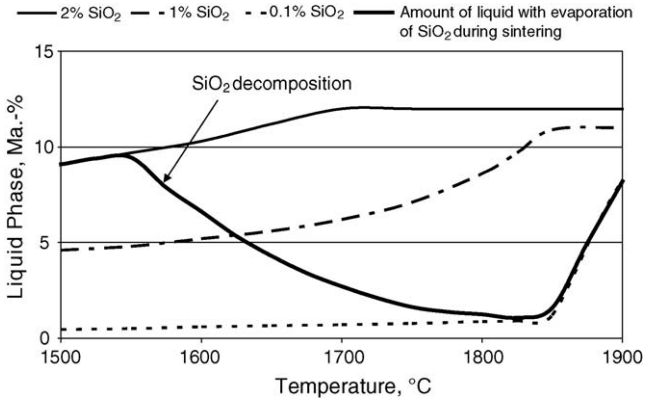

Fig. 7. Calculated amount of liquid phase in a LPSSiC material with 10 wt.% additives depending on the temperature and on the amount of existing SiO_2 in the material. The change of the amount of the liquid phase during sintering due to the evaporation is shown schematically.

In the investigation,[12] a maximum SiO-pressure was found at 1670–1700 °C. The data in 12 indicates that the evaporation of SiO_2 takes place predominantly in the temperature range 1500–1800 °C. The thermodynamic calculation and the experimental data[12] (Fig. 6a and b) showed that the SiO and CO partial pressure reduces after evaporation of the SiO_2.

The complex evaporation reaction of SiO_2 will also have an influence on the amount of liquid phase remaining during the densification process. This fact was not previously discussed in detail in the literature because the amount of liquid phase is difficult to determine. However, a thermodynamic calculation of the processes taking place during sintering can give a qualitative understanding of the processes. The net result is different grain boundary phases, which influence the density (Table 1), elastic constants (Fig. 5) and electrical properties of the GPS and HP materials.[23]

In Fig. 7, the thermodynamically calculated amounts of liquid phase, as a function of temperature, are given for different SiO_2-contents for the LPSSiC material with the Al_2O_3/Y_2O_3 ratio 5:3. The calculations show that a change of the SiO_2 content from 2 to 0.1 wt.% results in a more than 10 times decrease of the amount of liquid phase in the temperature range below 1800 °C. However, near the isothermal sintering temperatures, above 1900 °C, the amount of the liquid phase tends to the same value independent on the SiO_2-content. Due to the rapid decomposition of the SiO_2 at 1500–1750 °C the amount of liquid phase in the sample will change as schematically shown in Fig. 7, i.e. the amount of liquid phase decreases strongly during the heating of the sample from 1550 to 1800 °C. The vaporisation of the SiO_2 at relatively low temperatures results in the precipitation of the initially dissolved yttria alumina garnet ($Y_3Al_5O_{12}$) at intermediate temperatures during the heating cycle. Only near the isothermal sintering temperature (i.e. at the end of the heating cycle) does the YAG dissolve again in the liquid phase. The calculations also show that the amount of the liquid phase due to the SiO_2-content, strongly depends on the

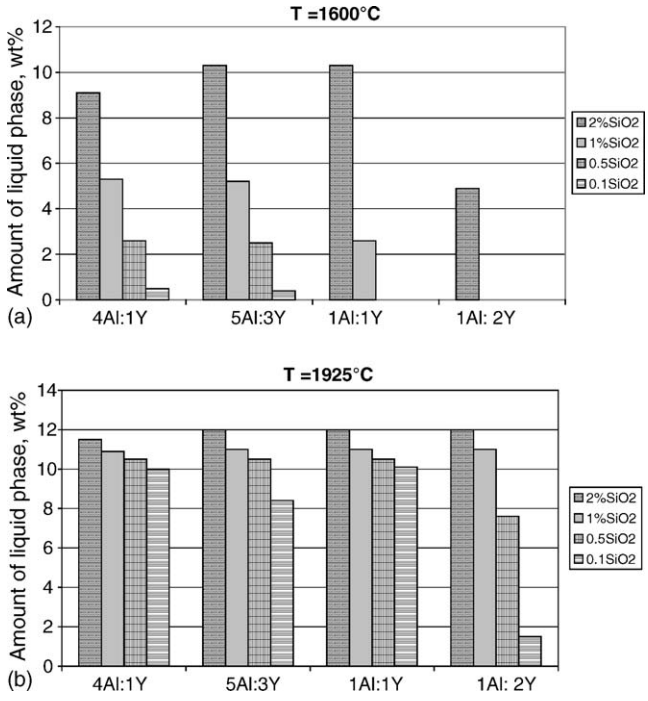

Fig. 8. Calculated amount of liquid phase in a material with 10 wt.% additives depending on the Al_2O_3/Y_2O_3 additive mol ratio at 1600 °C (a) and 1925 °C (b) for different SiO_2 content (amount in wt.%) in the additives (calculations were performed without any loss of matter by the gas phase).

Al_2O_3/Y_2O_3-ratio. In Fig. 8, the changes of the amount of the liquid phases for different Al_2O_3/Y_2O_3 ratios are given at both 1600 and 1925 °C. For the Al_2O_3 rich samples the dependence of the amount of liquid on the SiO_2-content is much less pronounced than for the samples with a higher Y_2O_3-content. This is one of the reasons for the bad densities observed for these GPS compounds. Therefore, slight changes in the weight loss of the materials by evaporation of SiO_2 and Al_2O_3, with a lower Al_2O_3/Y_2O_3 ratio, results in large deviations in the density and properties of the sintered body (Fig. 3).

The segregation observed during gas pressure sintering (Fig. 4) also reduces the densification. The fact that such segregations were observed only in the gas pressure sintered materials and not in the hot pressed materials suggest, that the segregation is also caused by the decrease of SiO_2-content. Details of this phenomenon are described in.[22]

The evaporation of the SiO_2, and therefore the decrease of the amount of liquid phase, will not take place homogeneously in the component, as it starts from the surfaces exposed to the sintering atmosphere. This can result in different shrinkage rates in different parts of the sintered body resulting in variations of the shape. This process is especially detrimental in samples with complicated shapes with large variations in the cross-sections. The dependence of the mass loss as a function of the Al_2O_3/Y_2O_3 ratio, shown in Fig. 3, is due to additional decomposition reaction i.e. the decomposition of the Al_2O_3. This reaction can be schematically

written as:[3,5,6]

$$4SiC\,(s) + 2Al_2O_3\,(s, l) \rightarrow 4CO\,(g) + SiO\,(g) + Al_2O\,(g) + 0.5Al\,(g) + 3Si\,(l) + 1.5Al\,(l) \quad (2)$$

At temperatures discussed (>1500° C) here Si and Al form one metallic melt. The amount of different products formed depends on the carbon activity caused by the residual carbon in the samples, the crucibles, C-heater and isolation, CO-activity and the ratio of the effective volume of the gas in the furnace to the sample volume during sintering. These reactions were investigated in several papers[3,5,6] and are also responsible for the high SiO-pressure in materials with little or no SiO_2 (compare Fig. 6a and b). An additional consequence of this decomposition is the shifting of the composition of the grain boundary towards the more rich Y_2O_3-side, which has a lower sintering activity due to formation of a reduced amount of liquid phase at low temperatures (see Figs. 3 and 8). These results show that a tight control of the interaction of the samples, with the surrounding atmosphere is a must for a reproducible sintering.

5. Conclusions

The densification of LPSSiC materials with a constant 10 wt.% of additives by conventional hot pressing and gas pressure sintering resulted in materials with very different grain boundary phases and physical properties. The hot pressed materials predominantly contain silicate and SiO_2-rich amorphous phases, whereas the gas pressure sintered materials have mainly yttrium aluminates as the grain boundary phase, indicating the evaporation losses of SiO_2 during gas pressure sintering in the temperature range 1500–1800 °C. The density and elastic constants of the dense hot pressed materials are somewhat lower than those for the porous free gas pressure sintered materials, due to the vaporisation of the SiO_2 and Al_2O_3 during gas pressure sintering.

Thermodynamic calculations of the composition of the gas phase formed during the sintering support the conclusion that there is extensive vaporisation of SiO_2 and changes in the precipitation process. Furthermore, the thermodynamically calculated amounts of the liquid, as a function of temperature, show that small changes in the SiO_2-content cause a strong reduction in the amount of liquid phase during sintering at 1500–1800 °C. The influence of the SiO_2 content on the amount of liquid formed is found to be more pronounced for low Al_2O_3/Y_2O_3 additives mol ratios.

References

1. Schwetz, K. A., Silicon carbide based hard materials. In *Handbook of Ceramic Hard Materials*, ed. R. Riedel. Wiley-VCH, Weinheim, 2000, pp. 683–748.
2. Omori, M. and Takei, H., Pressureless sintering of SiC. *J. Am. Ceram. Soc.*, 1982, **65**, C-92.
3. Ihle, J., Herrmann, M. and Adler, J., Phase formation in porous liquid phase sintered silicon carbide, Part I–IIII. *J. Eur. Ceram. Soc.*, 2005, **25**, 987–1013.
4. Grande, T., Sommerset, H., Hagen, E., Wiik, K. and Einarsrud, M.-A., Effect of weight loss on liquid-phase-sintered silicon carbide. *J. Am. Ceram. Soc.*, 1997, **80**, 1047–1052.
5. Baud, S., Thévenot, F. and Chatillon, C., High temperature sintering of SiC with oxide additives: IV: Powder beds and the influence of vaporization on the behaviour of SiC compacts. *J. Eur. Ceram. Soc.*, 2003, **23**, 29–36.
6. Baud, S., Thévenot, F., Pisch, A. and Chatillon, C., High temperature sintering of SiC with oxide additives: I. Analysis in the SiC-Al_2O_3 and SiC-Al_2O_3-Y_2O_3 systems. *J. Eur. Ceram. Soc.*, 2003, **23**, 1–8.
7. Misra, A. K., Thermochemical analysis of the silicon-carbide-alumina reaction with reference to liquid phase sintering of silicon carbide. *J. Am. Ceram. Soc.*, 1991, **74**, 345–351.
8. Mulla, M. A., Krstic, V. D. and Thompson, W. T., Reaction-inhibition during sintering of SiC with Al_2O_3 additions. *Canadian Metall. Quart.*, 1995, **34**, 357–362.
9. She, J. H. and Ueno, K., Effect of additive content on liquid-phase sintering on silicon carbide. *Mater. Res. Bull.*, 1999, **34**, 1629–1636.
10. Pujar, V. V., Jensen, R. P. and Padture, N. P., Densification of liquid-phase-sintered silicon carbide. *J. Mater. Sci. Lett.*, 2000, **19**, 1011–1014.
11. Winn, E. J. and Clegg, W. J., Role of the powder bed in the densification of silicon carbide sintered with yttria and alumina additives. *J. Am. Ceram. Soc.*, 1999, **82**, 3466–3470.
12. Schuesselbauer, E., Adler, J., Jaenicke-Roeßler, K. and Leitner, G., Sintering Investigations on LPS-SiC. In *Werkstoffwoche 98, Band VII*, 1999, pp. 207–212.
13. Padture, N. P. and Lawn, B. R., Toughness properties of a silicon carbide with an in situ induced heterogeneous grain structure. *J. Am. Ceram. Soc.*, 1994, **77**, 2518–2522.
14. Zhan, G.-D., Mitomo, M. and Kim, Y.-W., Microstructural control for strengthening of silicon carbide ceramics. *J. Am. Ceram. Soc.*, 1999, **82**, 924–926.
15. Kim, Y.-W., Kim, J.-Y., Rhee, S.-H. and Kim, D.-Y., Effect of initial particle size on microstructure of liquid-phase sintered silicon carbide. *J. Eur. Ceram. Soc.*, 2000, **20**, 945–949.
16. Joint Committee on Powder Diffraction Standards (JCPDS), ASTM, Swartmore, 2001.
17. Bale, C. W., Chartrand, P., Degterov, S. A., Eriksson, G., Hack, K., Ben Mahfoud, R. *et al.*, FactSage thermochemical software and databases. *Calphad*, 2002, **26**, 189–228.
18. SGPS—SGTE pure substances database, Scientific Group Thermodata Europe, 2000.
19. SGSL—SGTE alloy solutions database, Scientific Group Thermodata Europe, 1998.
20. 9288A00S—SGTE Si-Y-Al-C-O database, Scientific Group Thermodata Europe, 2000.
21. Groebner J., Constitution Calculations in the System Y-Al-Si-C-O, PhD Thesis, University of Stuttgart, Germany, 1994.
22. Can A., Herrmann M. and Ihle J., Segregation of additives during sintering of LPS SiC materials, in preparation.
23. Can A., McLachlan D.S., Sigalas J. and Herrmann M., Relationships between Microstructure and Electrical Properties of Liquid Phase sintered Silicon Carbide Materials using Impedance Spectroscopy, Paper on IX ECERS.
24. Grande, T., Sommerset, H. and Hagen, E., Effect of weight loss on liquid-phase-sintered silicon carbide. *J. Am. Ceram. Soc.*, 1997, **80**, 1047–1052.
25. Bondar, I. A. and Galakkov, F. Y., *Izv. Akad. Nauk, SSSR ser. Khimii.*, 1963, **7**, 1325.